Supporting Information for

Strong-motion Broadband Displacements from Collocated Ocean-bottom Pressure Gauges and Seismometers

A. Mizutani[1, 2], D. Melgar[2], K. Yomogida[1]

[1]Department of Earth and Planetary Sciences, Faculty of Sciences, Hokkaido University, Sapporo, Japan, [2]Department of Earth Sciences, University of Oregon, Eugene, Oregon, U.S.A.

Contents of this file

Introduction

Text S1 explains the details of the inversion methods in the main article. Fig. S1 shows the trade-off curves used to determine the weight in the inversion. Fig. S2 shows the displacement waveforms estimated by the proposed method at all the stations.

Text S1.

In the main text, we conducted three kinds of inversions: the tsunami source inversion (Section 2), the finite fault inversion (Section 5), and the joint inversion (Section 6). The first two solve the equation below:

$$\begin{bmatrix} d \\ 0 \end{bmatrix} = \begin{bmatrix} G \\ \alpha S \end{bmatrix} m, \tag{S1}$$

where d, G, S, and m are the data vector, kernel matrix, spatial smoothing matrix, and model vector, respectively. The weight parameter α is determined based on the trade-off curve of the variance reduction (VR) and model variance. In this study, the variance reduction is defined as (Takemura et al., 2018):

$$VR = \left(1 - \frac{\sum_i \int \left[u_i^{OBS}(t) - u_i^{SYN}(t) \right]^2 dt}{\sum_i \int [u_i^{OBS}(t)]^2 dt} \right) \times 100 \ [\%], \tag{S2}$$

where $u_i^{OBS}(t)$ and $u_i^{SYN}(t)$ are the observed and synthetic waveforms at station i. The trade-off curves of each result are shown in Fig. S1.

The tsunami source inversion is based on Kubota et al (2018). We first take the moving average with a time window of 60 sec and then apply a low-pass filter of 100 sec to the ocean-bottom pressure records. The time-derivative waveforms of them are used as the data and Green's functions. We set the record length to 25 min. The singular value decomposition is used to solve Eq. S1.

In the finite fault inversion, we solve Eq. 1 by the non-negative least squares method (Lawson & Hanson, 1995). For the tsunami data, we apply the same preprocessing as in the tsunami source inversion. For the displacement data, we apply a low-pass filter of 20 sec and use 30 sec from the origin time.

In the joint inversion, Eq. 1 is modified to:

$$\begin{bmatrix} d_{DIPS} \\ d_{TSUN} \\ 0 \end{bmatrix} = \begin{bmatrix} \dfrac{W_{DISP}}{N_{OBS}} G_{DISP} \\ \dfrac{W_{TSUN}}{N_{OBPG}} G_{TSUN} \\ \alpha S \end{bmatrix} m, \tag{S3}$$

where $\boldsymbol{d}_{DIPS}$, $\boldsymbol{G}_{DISP}$, and W_{DISP} are the data vector, kernel matrix, and weight for the displacement records; $\boldsymbol{d}_{TSUN}$, $\boldsymbol{G}_{TSUN}$, and W_{TSUN} are the same except that for the tsunami records; N_{OBS} and N_{OBPG} are the number of ocean-bottom seismometers and ocean-bottom pressure gauges. The preprocessing for data is the same as the above. The weights are also decided by the trade-off curve.
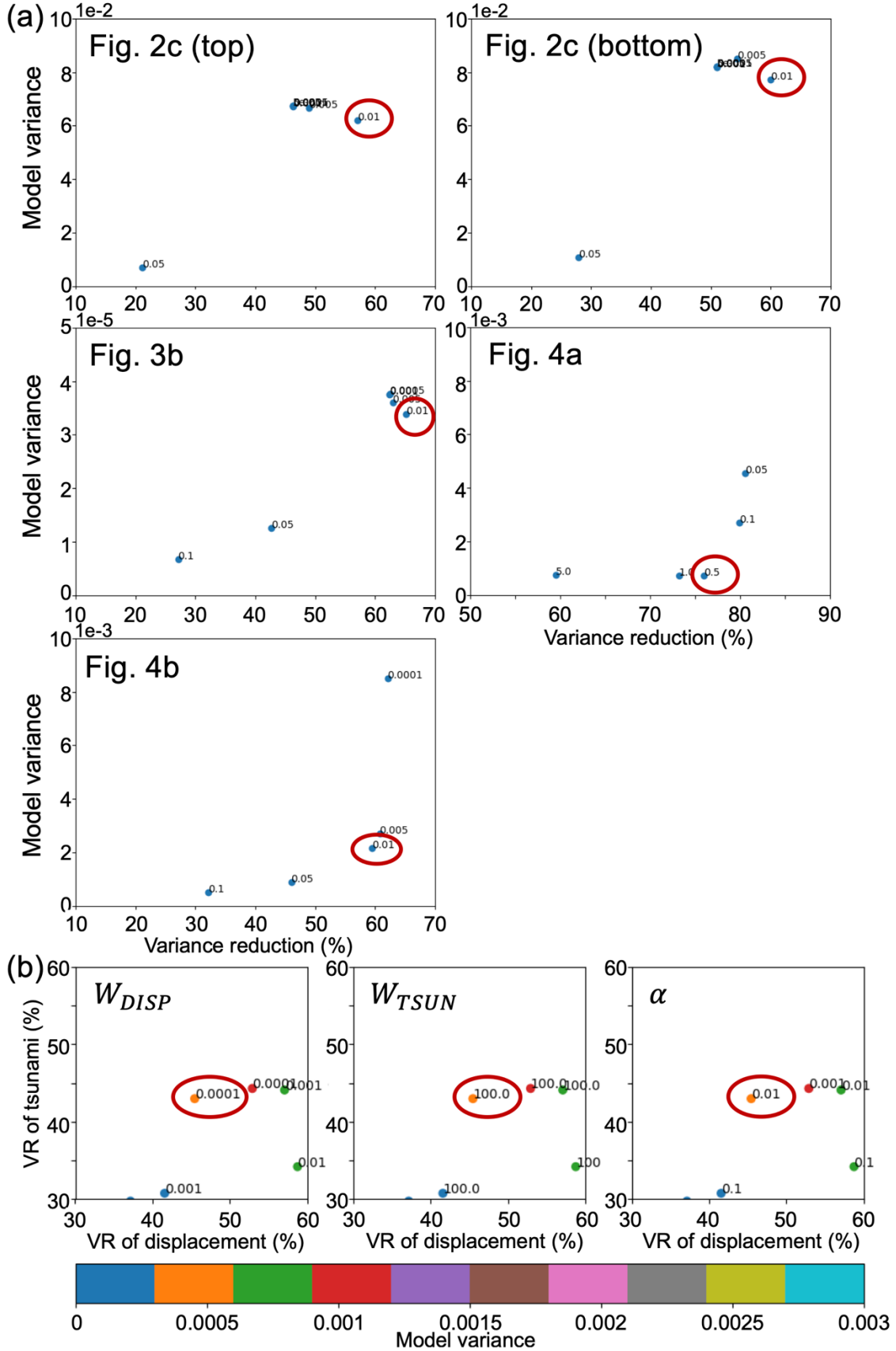
(a)

Fig. 2c (top)

Fig. 2c (bottom)

Fig. 3b

Fig. 4a

Fig. 4b

(b)

W_{DISP}

W_{TSUN}

α

Figure S1. (a) Trade-off curves used to determine the weight α in the inversions of Figs. 2c, 3b, 4a, and 4b. The text at each point is α in Eq. S1, and the red circles represent the weight we used. Note that although the result of Fig.4a comes from the bootstrap method, the trade-off curve is obtained by the single inversion. That is why the VR value is different from the main text. (b) Trade-off curves for the joint inversion (Fig. 4c). The left, center, and right panels are for W_{DIPS}, W_{TSUN}, and α in Eq. S3, respectively. The text and color of each point indicates the weight and model variance.
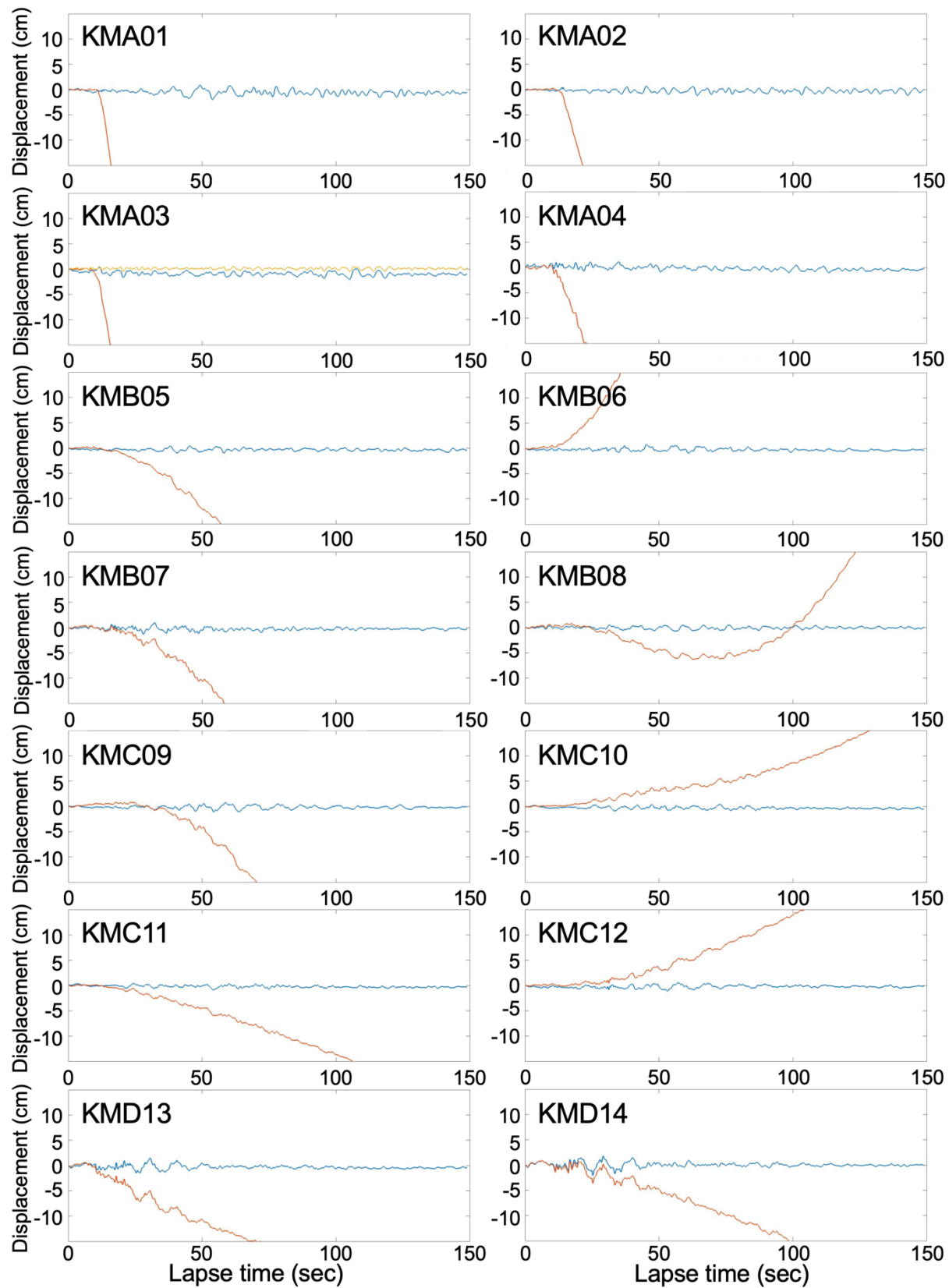
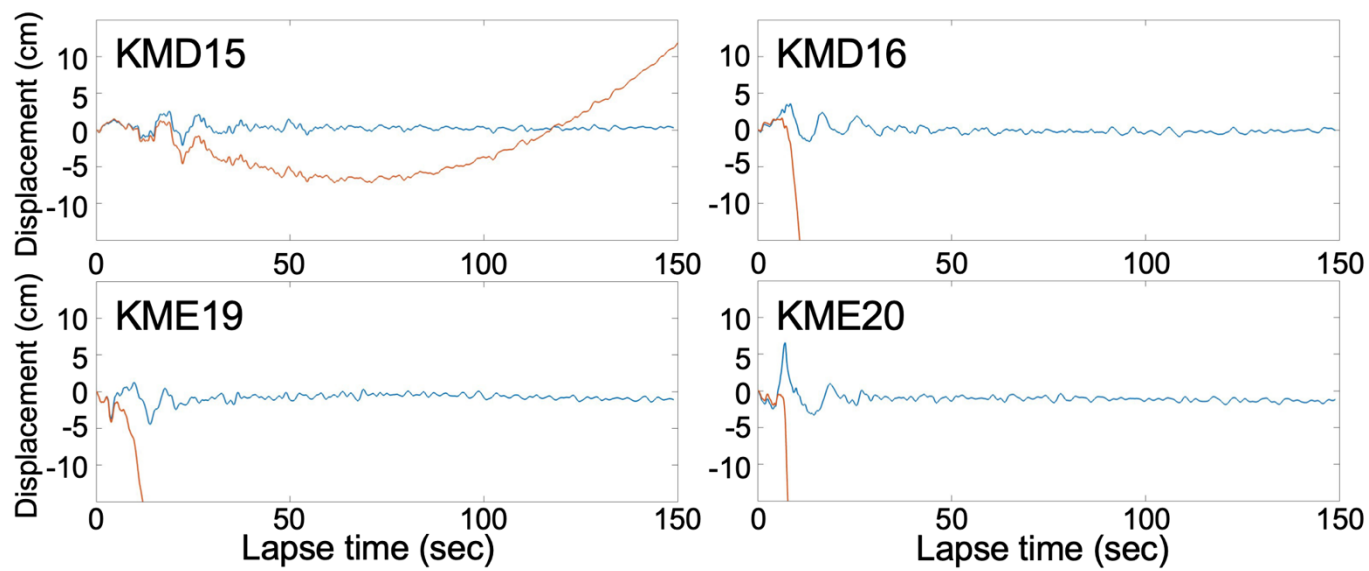**Figure S2.** Same as Fig. 3c except that at all other stations.

Figure S2. (Continued)

References

Kubota, T., Suzuki, W., Nakamura, T., Chikasada, N. Y., Aoi, S., Takahashi, N., & Hino, R. (2018). Tsunami source inversion using time-derivative waveform of offshore pressure records to reduce effects of non-tsunami components. *Geophysical Journal International*, *215*(2), 1200–1214. https://doi.org/10.1093/gji/ggy345

Lawson, C., & Hanson, R. (1995). *Solving least squares problems*. Society for Industrial and Applied Mathematics.

Takemura, S., Kimura, T., Saito, T., Kubo, H., & Shiomi, K. (2018). Moment tensor inversion of the 2016 southeast offshore Mie earthquake in the Tonankai region using a three-dimensional velocity structure model: Effects of the accretionary prism and subducting oceanic plate. *Earth, Planets and Space*, *70*(1), 50. https://doi.org/10.1186/s40623-018-0819-3